

# Performance Analysis of Flexible Ink-Jet Printed Humidity Sensors Based on Graphene Oxide

Dragana Z. Vasiljević<sup>1</sup>, Member, IEEE, Aida Mansouri, Luca Anzi, Roman Sordan,  
and Goran M. Stojanović, Member, IEEE

**Abstract**—This paper presents design, fabrication, and characterization of flexible capacitive graphene oxide (GO) based humidity sensors, which can be used in many applications, such as environmental protection, civil engineering, and agriculture. They consist of interdigitated electrodes ink-jet printed on a polyimide flexible substrate and GO based sensing layer. Measurement setup for testing and characterization was developed in laboratory conditions. The dependence of the capacitance and resistance of the GO based humidity sensors on the percentage of the applied humidity is presented. The main advantage of developed GO based capacitive humidity sensors is very large variation of capacitance, almost five orders of magnitude, compared with the previously demonstrated sensors. The other advantages of the sensors are fast response-recovery time, excellent reproducibility of the measurement results, and use of cost-effective additive ink-jet technology.

**Index Terms**—Capacitive sensor, graphene oxide, humidity sensor, ink-jet printing.

## I. INTRODUCTION

**D**UE to their high sensitivity, low power consumption, and fabrication costs, humidity sensors play an important role in many measurement and control applications, including meteorology, agriculture, industrial control, and medical instrumentation [1]–[4]. In the past years, a lot of effort has been made to develop high performance humidity sensors [5]–[8], exhibiting large sensitivity, fast response and recovery [9]–[10], and small humidity hysteresis. Various transduction techniques, such as capacitive, resistive, acoustic, optical and mechanical, have been adopted for the design of humidity sensors. Novel sensing materials, such as graphene oxide (GO), have recently been introduced in humidity sensors [11]–[21].

For instance, the sensitivity of complementary-metal-oxide-semiconductor (CMOS) interdigital capacitive humidity

sensors has been significantly improved by using GO as a sensing material [22]. However, some of the GO based sensors have been made by complex and costly fabrication techniques, such as etching [18] or layer-by-layer deposition [16]. The humidity sensors based on gold nanoparticles and GO have been fabricated by a combination of self-assembly and the sol-gel technique [23]. Spin-coating chemically derived GO on a quartz crystal microbalance have been used to fabricate humidity sensors in which the frequency response of the microbalance depended on the relative humidity (RH) [24]. Uniform GO films deposited by a dip-coating technique have been used for optical humidity sensing [12].

It has been widely acknowledged that ink-jet fabrication technology is a cost-effective method for manufacturing humidity sensors [25], [26]. Ink-jet printed GO has been used in temperature-modulated resistive humidity sensors which employ CMOS micro-electro-mechanical-system micro-hot-plate technology for the monitoring and control of indoor air quality [27]. Thin-film chemiresistors, made of a thin film composed of overlapped and reduced GO (rGO) platelets, were printed onto flexible plastic surfaces by using ink-jet technique [28]. However, in order to achieve the required sensitivity, the demonstrated sensors needed a large number of printed interdigitated electrodes on the substrates, i.e., a large area of the sensor chip.

Here we demonstrate GO based capacitive humidity sensors fabricated on flexible substrates, with very large variation of capacitance with percentage of applied RH. As a result of the extraordinary sensing properties of GO, the occupied area of the sensor chip was reduced with respect to the GO-free sensors which had more electrodes. The sensing was carried out for RH between 55 % and 95 %. The main advantage of the developed sensors compared to the previously demonstrated sensors is their remarkable sensitivity because the change of the measured capacitances was  $\sim 5$  orders of magnitude. The other advantages are fast response-recovery time, excellent reproducibility of the measurement results and use of cost-effective additive ink-jet technology, which allowed scalable production of the sensors. Mechanical flexibility of the sensors is also one of the very important advantages which allows installation of the sensor and measuring humidity in uneven and inaccessible places.

## II. DESIGN AND FABRICATION

The fabricated sensors were prepared by ink-jet printing process, using Dimatix deposition material printer (DMP-3000) and spin coating. An interdigitated capacitor with

Manuscript received March 6, 2018; revised March 29, 2018; accepted March 31, 2018. Date of publication April 5, 2018; date of current version May 9, 2018. This work was supported in part by the Central European Initiative (CEI) under Grant 1206.011-14 through CEI Know-How Exchange Program, in part by European Union H2020 Graphene Flagship Core 1 Project under Grant 696656, in part by the Provincial Secretariat for Higher Education and Science of the Province of Vojvodina under Project 142-451-2484/2017-01/01, and in part by the Ministry of Education, Science and Technological Development of Serbia within the Project TR32016. The associate editor coordinating the review of this paper and approving it for publication was Dr. Camilla Baratto. (Corresponding author: Dragana Z. Vasiljević.)

D. Z. Vasiljević and G. M. Stojanović are with the Faculty of Technical Sciences, University of Novi Sad, 21000 Novi Sad, Serbia (e-mail: vdragana@uns.ac.rs; sgoran@uns.ac.rs).

A. Mansouri, L. Anzi, and R. Sordan are with L-NESS, Department of Physics, Politecnico di Milano, Polo di Como, 22100 Como, Italy (e-mail: aida.mansouri@polimi.it; luca.anzi@polimi.it; roman.sordan@polimi.it).

Digital Object Identifier 10.1109/JSEN.2018.2823696

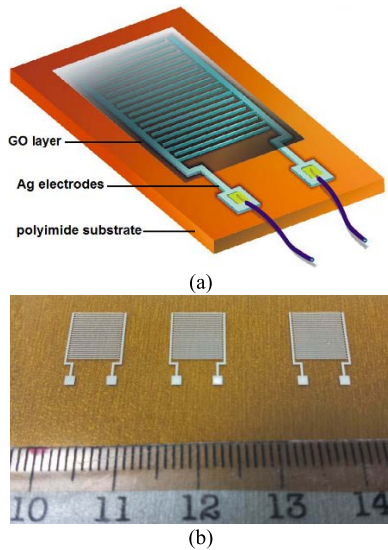


Fig. 1. Capacitive humidity sensor based on GO. (a) Schematic of the sensor. (b) Sensor's electrodes before deposition of GO. The ruler is in cm.

20 pairs of electrodes was designed, as shown in Fig. 1. It consists of a polyimide substrate, interdigitated Ag electrodes and sensing GO material.

The length of each electrode was 7 mm, while the electrode width and spacing were  $100\ \mu\text{m}$ , which was within the resolution limit of the used ink-jet printer. The first sensor layer was fabricated by printing commercially available Sun-Chemical Ag nanoparticle ink with 20 wt%. The thickness of the GTS polyimide film in the active area was  $75\ \mu\text{m}$  [29]. The resolution of the ink-jet process using DMP-3000 was mainly limited by the nozzle diameter (approximately equal to the droplet diameter) and the statistical variation of the droplet flight and spreading on the substrate. In case of printing with Ag nanoparticle ink, the minimum droplet diameter was  $\sim 36\ \mu\text{m}$ , and center-to-center drop spacing was  $18\ \mu\text{m}$ , which was obtained by changing the printhead angle [30]. Three structures with the same active area were printed and sintered at  $240\ ^\circ\text{C}$  for 30 min. Although the designed width of the electrodes was  $100\ \mu\text{m}$ , the printed lines shrunk to  $90\ \mu\text{m}$  after printing and  $\sim 80\ \mu\text{m}$  after sintering.

The second sensor layer was fabricated by spin coating 3 layers of commercially available Graphenea graphene oxide ink, with a concentration of 0.4 wt%, on top of the electrodes at 750 rpm for 5 s and then at 1500 rpm for 40 s. Monolayer content in the ink was  $>95\%$  at 0.05 wt%. The samples were dried at  $100\ ^\circ\text{C}$  for 30 min and then cooled to room temperature.

Proper deposition of GO was firstly verified by an optical microscope. Fig. 2 shows optical microscope images of sensor electrodes before and after spin coating of GO ink.

The presence of the GO flakes on top of the Ag electrodes is clearly visible in the latter case. The thickness of GO flakes was also verified by atomic force microscope (AFM) characterization, as it is shown in the same figure. The thickness of the GO flakes was  $\sim 9\ \text{nm}$  which confirmed successful deposition. The thickness of the Ag layer and the lateral dimensions of the flakes were  $\sim 400\ \text{nm}$  and  $\sim 10\ \mu\text{m}$ ,

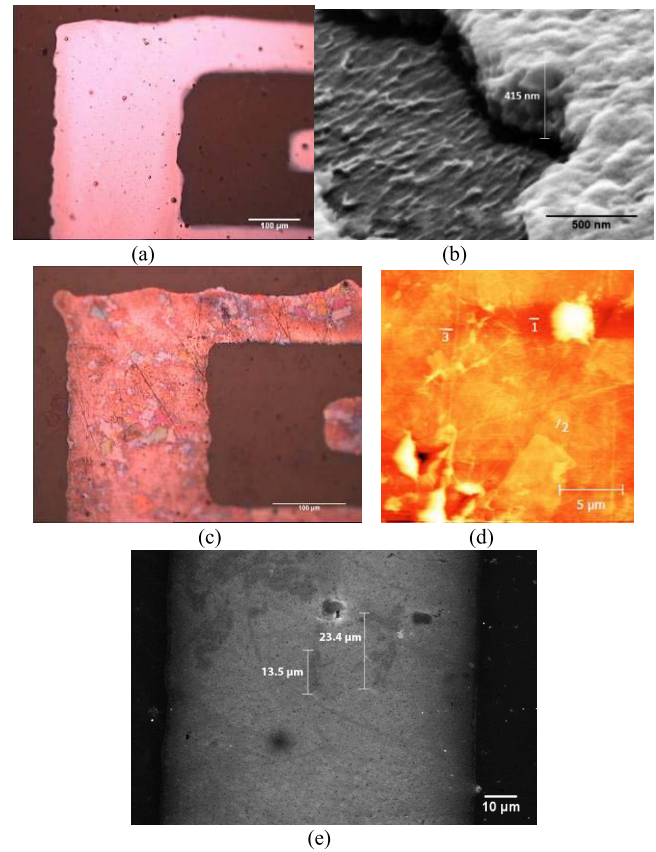


Fig. 2. Sensor Ag electrodes without and with the GO film. (a) An optical microscope image of bare sensor electrodes. (b) A tilted scanning electron microscope (SEM) image of a bare sensor electrode showing a typical thickness of  $\sim 400\ \text{nm}$  of the printed Ag layer. (c) An optical microscope image of sensor electrodes after spin coating GO ink. (d) An AFM image of the GO film deposited on the electrodes. A topography analysis along the sections 1, 2 and 3 indicated in the image reveals typical thickness of the GO flakes of  $\sim 9\ \text{nm}$ . (e) A top view SEM image of the sensor electrode showing a lateral dimension of deposited GO flakes of  $\sim 10\ \mu\text{m}$ .

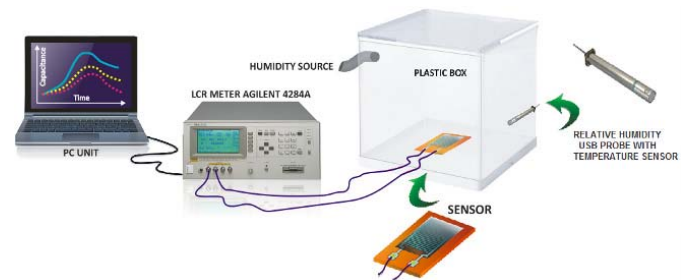


Fig. 3. Schematic of a humidity sensing measurement setup.

respectively, as shown in Fig. 2(b) and 2(e). The thickness of the GO layer was not uniform over the whole active area due to limitations of spin coating technology. AFM measurements showed multiple GO flakes agglomerated at some areas of the sensors.

Different geometries of the Ag electrodes were printed in order to understand whether they have influence on the spin coating of GO. We found that the spin coating process was mainly unaffected by the electrode design.

### III. RESULTS AND DISCUSSION

Measurements were performed using in-house measurement setup, illustrated in Fig. 3. It consists of a chamber

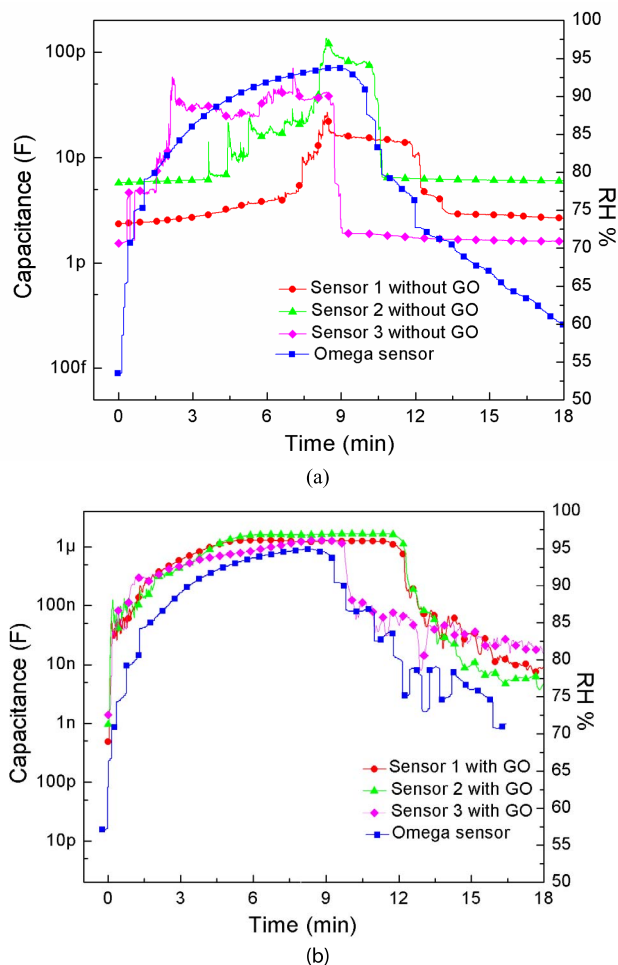


Fig. 4. Capacitance of 3 different sensors (encoded in different colors) as a function of time. (a) Sensors without the GO film. (b) Sensors with the GO film. In both cases humidity was changed from 55 %RH to 95 %RH and then back to 55 %RH. The blue curves (with the scale on the right) show the RH measured by the commercial sensor at the same time.

(plastic box) and humidity source (aerosol). Capacitance and resistance of the fabricated sensors were measured using Agilent LCR meter 4284A. Commercially available Omega RH USB probe with a temperature sensor was also placed in the chamber and used as a reference [31].

The capacitance and resistance of all 3 sensor samples were measured as a function of time while changing the RH as follows. The sensor was placed in the chamber with laboratory atmosphere at room temperature, and its stable output was recorded. The humidity source was then turned on and it was kept running for 9 min after which the steady state with 95 %RH was reached, as determined by the commercial sensor placed in the same chamber. Finally, the humidity source was turned off and the sensor was exposed to laboratory atmosphere again. The measurements were initially performed at three different frequencies: 1, 10 and 100 kHz. The highest sensitivity was obtained at 1 kHz, which was then used in all present measurements. Fig. 4(a) shows the results obtained by measuring the capacitance of the sensors, without and with the GO film, under such conditions. In sensors without the GO film, the capacitance increased  $\sim 10$  times in the humidity range from 55 %RH to 95 %RH, but it did not exceed

120 pF. However, in sensors with the GO film, Fig. 4(b), the capacitance increased by almost five orders of magnitude, from 43 pF to 1.6  $\mu$ F, in the same humidity range. The difference in the Omega sensor response, which can be observed by comparing Fig. 4(a) and (b), is a consequence of the drying process which was simply done by exposing the sensors to ambient air. This probably left some residual humidity in the sensing area of the Omega sensor.

The obtained results can be explained by the expression for the capacitance of the sensing material [32].

$$C = \varepsilon^* C_0 = \left( \varepsilon_r - \frac{i\gamma}{\omega \varepsilon_0} \right) C_0 \quad (1)$$

where  $\varepsilon^*$  is the complex dielectric constant of the material,  $C_0$  is the capacitance of the vacuum capacitor with the same dimensions as the sensing layer,  $\varepsilon_r$  is the relative dielectric constant of the material,  $\varepsilon_0$  is the vacuum permittivity,  $\gamma$  is the leak conductance, and  $\omega$  is the angular frequency. This shows that the capacitance of the sensing material is proportional to  $\gamma$ . With the increase of RH, water molecules are physisorbed through single hydrogen bonding on the hydroxyl groups in GO [11]. When exposed to the external electric field, the water molecules undergo protonation (due to a transfer of oxygen from the large number of oxygen-containing groups in GO, e.g., epoxy groups) and yield a large number of hydronium ions ( $H_3O^+$ ) which act as charge carriers [11]. Because of this, the increase of RH increases  $\gamma$  which increases the capacitance. A very good sensitivity, observed here at large RH, is due to the physisorbed water layers behaving as liquid which allows hydronium ions to freely move and contribute to the ionic conduction [11]. Large surface area of the GO flakes is also beneficial for increasing the sensitivity of the sensors, which ultimately depends on the film thickness and its uniformity. For instance, we found that the GO film was not uniform over the entire active area due to the limitations of the spin coating process. Agglomerates of the GO flakes were found in many places leading to the increase of sensitivity. The different humidity response of different sensors can also be attributed to the nonuniformity of the GO film.

Fig. 5 shows the time dependence of the resistance of the fabricated GO sensors recorded at the same time as the capacitances shown in Fig. 4(b). In the previous reports [33], the change of resistance has been from 300 k $\Omega$  to 20 k $\Omega$  over the humidity range from 45% to 85%. In our work, the obtained resistance change was in the range from 2.5 M $\Omega$  to 5 k $\Omega$  under the same conditions.

Long term stability measurements were performed for all three sensors after 21 months from their fabrication. The measurements showed a decrease of capacitance response by an order of magnitude, which is not that significant considering their total response.

Response and recovery time is one of the most important figures of merit of humidity sensors, especially in commercial settings. Fig. 4(b) and 5 also show the response–recovery characteristics of the GO based humidity sensors. The time taken by a sensor to reach 90 % of the final capacitance change was defined as the response time in the case of adsorption and recovery time in the case of desorption. The measured

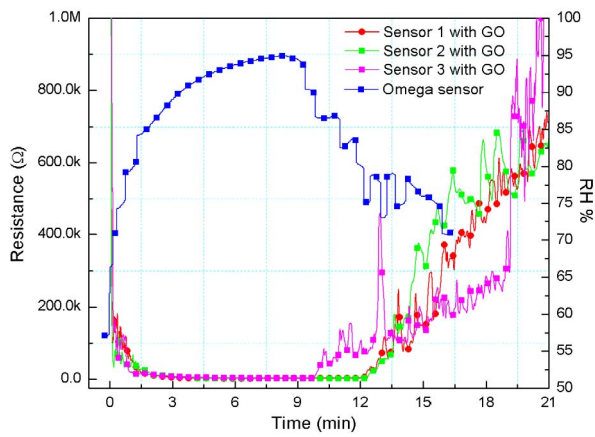


Fig. 5. Resistance of 3 different sensors (encoded in different colors) with GO as sensing material. The resistances were measured at the same time as the capacitance of the sensors shown in Figure 4b. The blue curve (with the scale on the right) shows RH measured by the commercial sensor at the same time.

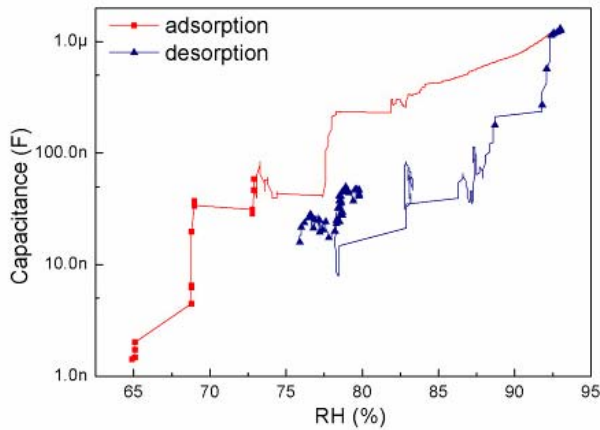


Fig. 6. Humidity hysteresis curves of the GO based sensor.

average response and recovery times were 30 s and 150 s, respectively, for all fabricated sensors. This could be explained by different speeds at which the humidity was introduced and removed from the chamber (i.e., the plastic box depicted in Fig. (3)). The humidity was introduced into the chamber by an aerosol device, whereas the humidity exhaustion was performed by self-drying in laboratory atmosphere, similar to previous reports [13]. However, the realized sensor had much higher sensitivity. The rapid response–recovery behavior benefited from the porous structure, hydrophilic functional groups, and large inter-layer space of the GO film.

Hysteresis is one of the most important performance metrics of humidity sensors. Hysteresis leads to the measurement errors because different capacitances (i.e., RH readouts) could be obtained at the same RH depending on whether RH increases or decreases. Fig. 6 shows the hysteresis curve in the adsorption and desorption phase of the fabricated GO sensors. The humidity hysteresis characteristic of the sensors was measured by increasing the RH from 55% to 95% and then decreasing the RH back to 55%. RH was measured by the commercial sensor which has a hysteresis width

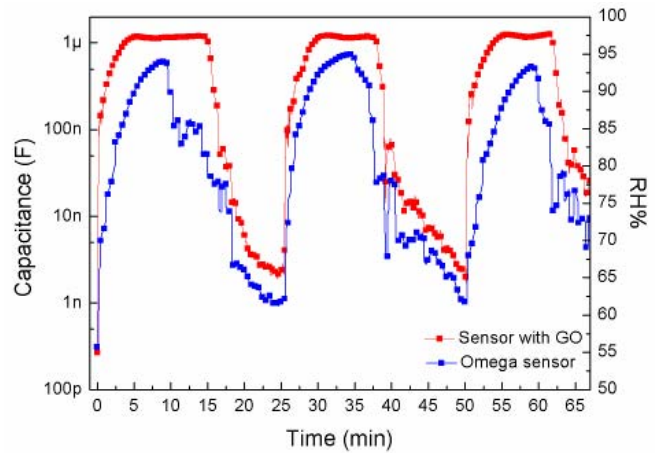


Fig. 7. Repeatability of the GO sensors compared to a commercial sensor (with scale on the right) over three response/recovery cycles.

TABLE I  
PERFORMANCE OF THE SENSORS PRESENTED IN THIS WORK  
COMPARED TO THE STATE-OF-THE-ART SENSORS

Sensing material	Fabrication method	Measurement range (%RH) <sup>a</sup>	Sensitivity (pF/%RH)	Reference
GO	Ink-jet printing	55-95	40000	this work
ZnO	CMOS+ post process	40-90	3.18	[4]
GO	Drop casting	15-95	46.25	[5]
rGO/SnO <sub>2</sub>	Hydro thermal synthesis	11-97	1604.89	[18]
GO/MWCNT	magnetron sputtering + drop casting	11-97	7980	[19]
GO/PDDA	LbL self-assembly	11-97	1552.3	[20]
GO	Simulation	0-100	7680	[21]

$\Delta RH \sim \pm 1\%$ . The maximum hysteresis width of the fabricated sensors was  $\Delta RH \sim 10\%$ . This indicates that further improvements would be needed if the high sensitivity of the presented sensors were to be used in commercial applications.

Fig. 7 shows the repeatability measurement of one of the fabricated GO sensors. The repeatability of the GO sensors was tested by exposing the sensors to three alternating RH cycles between 55%RH and 95%RH. During the response/recovery cycles, the capacitance response was highly repeatable demonstrating the advantage of the sensors in possible sensor applications. The fabricated sensors compared favorably to the used commercial sensor both in terms of repeatability and sensing performances.

Sensitivity ( $S$ ) used to characterize the sensor performance is defined as:

$$S = \frac{\Delta C}{\Delta RH} \quad (2)$$

where  $\Delta C$  is the sensor response change of capacitance and  $\Delta RH$  is the RH change. In the present case, the sensitivity

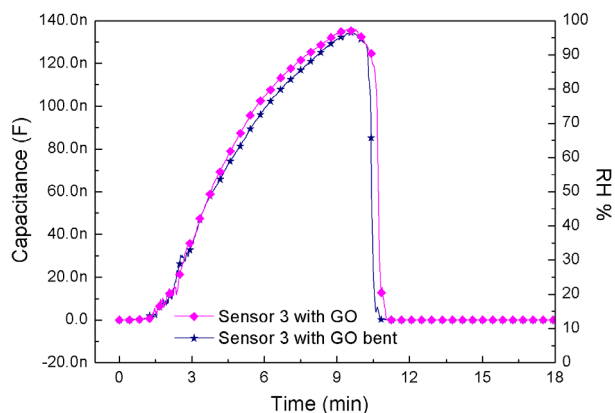


Fig. 8. The humidity measurements performed on one of the sensors without (the magenta line) and with (the blue line) bending.

was  $\sim 40$  nF/%RH. The sensing properties of the proposed sensor are comparable to previously demonstrated capacitive-type humidity GO sensors realized in different technologies [11], [17]–[20], [23], [24] or with different sensing materials [4], [25]. The main advantage of the presented sensor is its very large change of capacitance with humidity, as shown in Table 1. The fabrication procedure was also found to provide a reproducible sensing property which is of the utmost importance in the possible applications of the realized sensors.

The influence of bending on sensors response was also investigated. Sensors were bent around a cylinder with a radius of 3.5 mm encompassing an angle of  $120^\circ$  and exposed to the same humidity tests. The obtained results were almost identical compared to that without bending, as shown in Fig. 8. This represents an important advantage of the proposed sensors for simple monitoring of humidity because they can be placed on almost any surface without affecting their response.

#### IV. CONCLUSION

The capacitive interdigitated GO based humidity sensors were fabricated on flexible foil by combining ink-jet printing and spin coating. The sensors comprised interdigitated electrodes made by ink-jet printing of Ag nanoparticle ink and a sensing layer made by spin coating of GO ink. Application of additive ink-jet printing process reduced costs and provided good mechanical properties. Flexible substrate and GO used in the presented sensors enable simple monitoring of humidity in various environments. The humidity sensing properties of the fabricated GO based sensors were investigated by exposing the sensors to humidity in the range 55–95 %RH at room temperature. The sensors exhibited excellent sensitivity in the investigated range of humidity, changing the capacitance by almost 5 orders of magnitude (from 43 pF to  $1.6 \mu\text{F}$ ).

#### REFERENCES

[1] L. Gu, Q.-A. Huang, and M. Qin, "A novel capacitive-type humidity sensor using CMOS fabrication technology," *Sens. Actuators B, Chem.*, vol. 99, nos. 2–3, pp. 491–498, May 2004, doi: [10.1016/j.snb.2003.12.060](https://doi.org/10.1016/j.snb.2003.12.060).

[2] M. Maksimovic *et al.*, "Application of a LTCC sensor for measuring moisture content of building materials," *Construction Building Mater.*, vol. 26, no. 1, pp. 327–333, 2012, doi: [10.1016/j.conbuildmat.2011.06.029](https://doi.org/10.1016/j.conbuildmat.2011.06.029).

[3] A. Oprea, J. Courbat, N. Bărsan, D. Briand, N. F. De Rooij, and U. Weimar, "Temperature, humidity and gas sensors integrated on plastic foil for low power applications," *Sens. Actuators B, Chem.*, vol. 140, no. 1, pp. 227–232, 2009, doi: [10.1016/j.snb.2009.04.019](https://doi.org/10.1016/j.snb.2009.04.019).

[4] M.-Z. Yang, C.-L. Dai, and C.-C. Wu, "Sol-gel zinc oxide humidity sensors integrated with a ring oscillator circuit on-a-chip," *Sensors*, vol. 14, no. 11, pp. 20360–20371, 2014, doi: [10.3390/s141120360](https://doi.org/10.3390/s141120360).

[5] T. Qiang *et al.*, "High-performance porous MIM-type capacitive humidity sensor realized via inductive coupled plasma and reactive-ion etching," *Sens. Actuators B, Chem.*, vol. 258, pp. 704–714, Apr. 2018, doi: [10.1016/j.snb.2017.11.060](https://doi.org/10.1016/j.snb.2017.11.060).

[6] M. Sasikumar and N. P. Subiramaniam, "Microstructure, electrical and humidity sensing properties of  $\text{TiO}_2$ /polyaniline nanocomposite films prepared by sol-gel spin coating technique," *J. Mater. Sci., Mater. Electron.*, pp. 1–8, Jan. 2018, doi: [10.1007/s10854-018-8697-9](https://doi.org/10.1007/s10854-018-8697-9).

[7] Z. Wang, X. Fan, C. Li, G. Men, D. Han, and F. Gu, "Humidity-sensing performance of 3DOM  $\text{WO}_3$  with controllable structural modification," *ACS Appl. Mater. Interfaces*, vol. 10, no. 4, pp. 3776–3783, 2018, doi: [10.1021/acsami.7b17048](https://doi.org/10.1021/acsami.7b17048).

[8] J. Zhao *et al.*, "Highly sensitive  $\text{MoS}_2$  humidity sensors array for non-contact sensation," *Adv. Mater.*, vol. 29, no. 34, 2017, Art. no. 1702076, doi: [10.1002/adma.201702076](https://doi.org/10.1002/adma.201702076).

[9] Z. Duan, M. Xu, T. Li, Y. Zhang, and H. Zou, "Super-fast response humidity sensor based on  $\text{La}_{0.7}\text{Sr}_{0.3}\text{MnO}_3$  nanocrystals prepared by PVP-assisted sol-gel method," *Sens. Actuators B, Chem.*, vol. 258, pp. 527–534, Apr. 2018, doi: [10.1016/j.snb.2017.11.169](https://doi.org/10.1016/j.snb.2017.11.169).

[10] B. Gu, C. Ye Aung, P. H. J. Chong, Y. L. Guan, and K.-T. Yong, "Reversible and fast responsive optical fiber relative humidity sensor based on polyelectrolyte self-assembly multilayer film," *IEEE Sensors J.*, vol. 18, no. 3, pp. 1081–1086, Feb. 2018, doi: [10.1109/JSEN.2017.2776398](https://doi.org/10.1109/JSEN.2017.2776398).

[11] H. Bi *et al.*, "Ultrahigh humidity sensitivity of graphene oxide," *Sci. Rep.*, vol. 3, Sep. 2013, Art. no. 2714, doi: [10.1038/srep02714](https://doi.org/10.1038/srep02714).

[12] H. Chi, Y. J. Liu, F. Wang, and C. He, "Highly sensitive and fast response colorimetric humidity sensors based on graphene oxides film," *ACS Appl. Mater. Interfaces*, vol. 7, no. 36, pp. 19882–19886, 2015, doi: [10.1021/acsami.5b06883](https://doi.org/10.1021/acsami.5b06883).

[13] Y. Yao, X. Chen, H. Guo, Z. Wu, and X. Li, "Humidity sensing behaviors of graphene oxide-silicon bi-layer flexible structure," *Sens. Actuators B, Chem.*, vol. 161, no. 1, pp. 1053–1058, 2012, doi: [10.1016/j.snb.2011.12.007](https://doi.org/10.1016/j.snb.2011.12.007).

[14] L. Guo *et al.*, "Two-beam-laser interference mediated reduction, patterning and nanostructuring of graphene oxide for the production of a flexible humidity sensing device," *Carbon*, vol. 50, pp. 1667–1673, Apr. 2012, doi: [10.1016/j.carbon.2011.12.011](https://doi.org/10.1016/j.carbon.2011.12.011).

[15] P.-G. Su and Z.-M. Lu, "Flexibility and electrical and humidity-sensing properties of diamine-functionalized graphene oxide films," *Sens. Actuators B, Chem.*, vol. 211, pp. 157–163, May 2015, doi: [10.1016/j.snb.2015.01.089](https://doi.org/10.1016/j.snb.2015.01.089).

[16] D. Zhang, J. Tong, and B. Xia, "Humidity-sensing properties of chemically reduced graphene oxide/polymer nanocomposite film sensor based on layer-by-layer nano self-assembly," *Sens. Actuators B, Chem.*, vol. 197, pp. 66–72, Jul. 2014, doi: [10.1016/j.snb.2014.02.078](https://doi.org/10.1016/j.snb.2014.02.078).

[17] R. Gao, D.-F. Lu, J. Cheng, Y. Jiang, L. Jiang, and Z. M. Qi, "Humidity sensor based on power leakage at resonance wavelengths of a hollow core fiber coated with reduced graphene oxide," *Sens. Actuators B, Chem.*, vol. 222, pp. 618–624, Jan. 2016, doi: [10.1016/j.snb.2015.08.108](https://doi.org/10.1016/j.snb.2015.08.108).

[18] D. Zhang, H. Chang, P. Li, R. Liu, and Q. Xue, "Fabrication and characterization of an ultrasensitive humidity sensor based on metal oxide/graphene hybrid nanocomposite," *Sens. Actuators B, Chem.*, vol. 225, pp. 233–240, Mar. 2016, doi: [10.1016/j.snb.2015.11.024](https://doi.org/10.1016/j.snb.2015.11.024).

[19] X. Li, X. Chen, X. Chen, X. Ding, and X. Zhao, "High-sensitive humidity sensor based on graphene oxide with evenly dispersed multi-walled carbon nanotubes," *Mater. Chem. Phys.*, vol. 207, pp. 135–140, Mar. 2018, doi: [10.1016/j.matchemphys.2017.12.033](https://doi.org/10.1016/j.matchemphys.2017.12.033).

[20] D. Zhang, J. Tong, B. Xia, and Q. Xue, "Ultrahigh performance humidity sensor based on layer-by-layer self-assembly of graphene oxide/polyelectrolyte nanocomposite film," *Sens. Actuators B, Chem.*, vol. 203, pp. 263–270, Nov. 2014, doi: [10.1016/j.snb.2014.06.116](https://doi.org/10.1016/j.snb.2014.06.116).

- [21] R. Guo, W. Tang, C. Shen, and X. Wang, "High sensitivity and fast response graphene oxide capacitive humidity sensor with computer-aided design," *Comput. Mater. Sci.*, vol. 111, pp. 289–293, Jan. 2016, doi: [10.1016/j.commatsci.2015.09.032](https://doi.org/10.1016/j.commatsci.2015.09.032).
- [22] C.-L. Zhao, M. Qin, W.-H. Li, and Q.-A. Huang, "Enhanced performance of a CMOS interdigital capacitive humidity sensor by graphene oxide," in *Proc. Solid-State Sens., Actuators Microsyst. Conf. (TRANSDUCERS)*, vol. 16, Jun. 2011, pp. 1954–1957, doi: [10.1109/TRANSDUCERS.2011.5969243](https://doi.org/10.1109/TRANSDUCERS.2011.5969243).
- [23] P.-G. Su, W.-L. Shiu, and M.-S. Tsai, "Flexible humidity sensor based on Au nanoparticles/graphene oxide/thiolated silica sol-gel film," *Sens. Actuators B, Chem.*, vol. 216, pp. 467–475, Sep. 2015, doi: [10.1016/j.snb.2015.04.070](https://doi.org/10.1016/j.snb.2015.04.070).
- [24] Y. Yao, X. Chen, H. Guo, and Z. Wu, "Graphene oxide thin film coated quartz crystal microbalance for humidity detection," *Appl. Surf. Sci.*, vol. 257, pp. 7778–7782, Sep. 2011, doi: [10.1016/j.apsusc.2011.04.028](https://doi.org/10.1016/j.apsusc.2011.04.028).
- [25] F. Molina-Lopez, D. Briand, and N. F. de Rooij, "All additive inkjet printed humidity sensors on plastic substrate," *Sens. Actuators B, Chem.*, vols. 166–167, pp. 212–222, May 2012, doi: [10.1016/j.snb.2012.02.042](https://doi.org/10.1016/j.snb.2012.02.042).
- [26] J. Weremczuk, G. Tarapata, and R. Jachowicz, "Humidity sensor printed on textile with use of ink-jet technology," *Proc. Eng.*, vol. 47, pp. 1366–1369, Dec. 2012, doi: [10.1016/j.proeng.2012.09.410](https://doi.org/10.1016/j.proeng.2012.09.410).
- [27] A. De Luca *et al.*, "Temperature-modulated graphene oxide resistive humidity sensor for indoor air quality monitoring," *Nanoscale*, vol. 8, no. 8, pp. 4565–4572, 2016, doi: [10.1039/c5nr08598e](https://doi.org/10.1039/c5nr08598e).
- [28] V. Dua *et al.*, "All-organic vapor sensor using inkjet-printed reduced graphene oxide," *Angew. Chem. Int. Ed.*, vol. 49, no. 12, pp. 2154–2157, 2010, doi: [10.1002/anie.200905089](https://doi.org/10.1002/anie.200905089).
- [29] GTS Flexible Materials Ltd. *Electronics*. Accessed: Nov. 20, 2017. [Online]. Available: <http://www.gts-flexible.com/home/>
- [30] Dimatix Inc. *Dimatix Materials Printer DMP-3000*. Accessed: Jun. 7, 2017. [Online]. Available: <http://www.dimatix.com>
- [31] *OMEGA Humidity Probe*. Accessed: Nov. 20, 2017. [Online]. Available: <http://www.omega.com/>
- [32] Q. Wang, Y. Z. Pan, S. S. Huang, S. T. Ren, P. Li, and J. J. Li, "Resistive and capacitive response of nitrogen-doped TiO<sub>2</sub> nanotubes film humidity sensor," *Nanotechnology*, vol. 22, no. 2, p. 025501, 2010, doi: [10.1088/0957-4484/22/2/025501](https://doi.org/10.1088/0957-4484/22/2/025501).
- [33] G. Naik and S. Krishnaswamy, "Room-temperature humidity sensing using graphene oxide thin films," *Graphene*, vol. 5, no. 1, pp. 1–13, 2016, doi: [10.4236/graphene.2016.51001](https://doi.org/10.4236/graphene.2016.51001).



**Dragana Z. Vasiljević** was born in Dobož, Bosnia and Herzegovina. She received the B.Sc. and M.Sc. degrees in electrical engineering from the University of Novi Sad, Novi Sad, Serbia, in 2010, where she is currently pursuing the Ph.D. degree with the Laboratory for Nano and Printed Electronics, Faculty of Technical Sciences. Her research is mainly focused on design, fabrication, and characterization of different type of flexible/organic/printed sensors and characterization of nanomaterials appropriate for sensing applications.



**Aida Mansouri** was born in Tehran, Iran. She received the degree from the Azad University of Saveh in 2010, the double M.Sc. degrees in innovation and sustainability from the Politecnico di Milano and Alta Scuola Politecnica, and the Ph.D. degree from Politecnico di Milano in 2017, all in electronic engineering. She started the Post-Doctoral Program with Politecnico di Milano. Her current research is focused on the integration of graphene in nanoelectronic devices and circuits.



**Luca Anzi** was born in Italy in 1988. He received the B.E. degree in computer science engineering, the M.Sc. degree in materials engineering and nanotechnology, and the Ph.D. degree in physics from the Politecnico di Milano, Italy, in 2011, 2014, and 2018, respectively. Since 2018, he has been a Post-Doctoral Research Fellow with the Nanoscale Devices Group, the Department of Physics, Politecnico di Milano. His main area of research interest includes graphene and other 2-D materials for nanoelectronic devices.



**Roman Sordan** received the Ph.D. degree in solid state physics from the University of Belgrade, Serbia, in 1999. He was with the Max Planck Institute for Solid State Research in Stuttgart, Germany. He is an Associate Professor of Physics with Politecnico di Milano, Italy. His current research interests include the integration of graphene and other 2-D materials in nanoelectronic devices and circuits.



**Goran M. Stojanović** (M'04) was born in Smederevo, Serbia, in 1972. He received the B.Sc., M.Sc., and Ph.D. degrees in electrical engineering from the University of Novi Sad, Novi Sad, Serbia, in 1996, 2003, and 2005, respectively. He is currently a Full Professor with the Faculty of Technical Sciences, University of Novi Sad. He has authored or co-authored 180 scientific papers including 58 articles in leading international peer-reviewed journals (with impact factors). His research interest includes printed/organic/flexible electronics and nanoelectronics and application of advanced nanostructured materials. He is a reviewer of many leading international journals. He has almost ten years of experience in coordination and implementation of different EU funded projects.